Histol Histopathol (2022) 37: 513-526

http://www.hh.um.es

Histology and Histopathology
From Cell Biology to Tissue Engineering

ORIGINAL ARTICLE **Open Access**

Circ_0044520 regulates the progression of laryngeal squamous cell carcinoma via the miR-338-3p/ROR2 axis

Huijun Yang, Gang Yu, Yan Wang and Xing Guo

Department of Otolaryngology, First Affiliated Hospital of China Medical University, Shenyang City, Liaoning, China

Summary. Background. Laryngeal squamous cell carcinoma (LSCC) is the second most common malignant tumor in head and neck. Circular RNA_0044520 (circ_0044520) expression is increased in LSCC. However, the molecular mechanism of circ_0044520 remains unknown.

Methods. The expression of circ_0044520, microRNA-338-3p (miR-338-3p) and receptor tyrosine kinase-like orphan receptor 2 (ROR2) were detected by quantitative real-time fluorescence polymerase chain reaction (qRT-PCR). Cell viability, cell proliferation and apoptosis were detected by Cell Counting Kit-8 (CCK-8) assay, colony formation assay and flow cytometry assay, respectively. Western blot examined the protein levels of PCNA, Cyclin D1, Bax, Bcl-2 and ROR2 cells. The relationship between miR-338-3p and circ_0044520 or ROR2 was verified by Dual-luciferase reporter assays. The xenotransplantation model was established to study the role of circ_0044520 in vivo.

Results. The expression of circ_0044520 and ROR2 was increased in LSCC tissues and cells, while the expression of miR-338-3p was decreased. Circ_0044520 can sponge miR-338-3p, and ROR2 is the target of miR-338-3p. In vitro complement experiments showed that knockdown of circ_0044520 significantly inhibited malignant behavior of LSCC, while co-transfection of miR-338-3p inhibitor partially up-regulated this change. In addition, miR-338-3p can inhibit the proliferation of LSCC cells, while co-transfection of overexpression of ROR2 can partially reverse this change. Mechanically, circ_0044520 regulates ROR2 expression in LSCC cells by sponging miR-338-3p. In addition, in vivo studies have shown that down-regulation of circ_0044520 inhibits tumor growth.

Conclusion. Circ_0044520 silencing plays anti-proliferation and pro-apoptosis roles in LSCC cells by regulating the miR-338-3p/ROR2 axis, suggesting that the circ_0044520/miR-338-3p/ROR2 axis may be a potential regulatory mechanism for the treatment of LSCC.

Key words: Circ_0044520, miR-338-3p, ROR2, LSCC

Introduction

Laryngeal cancer is a common malignant tumor of the head and neck, mostly occurring in men (Steuer et al., 2017). In recent years, the incidence and mortality of laryngeal cancer have been on the rise. The most common type of laryngeal cancer is laryngeal squamous carcinoma (LSCC), which accounts for approximately 90% of all laryngeal cancers (Siegel et al., 2015). It has the characteristics of difficult diagnosis and low survival rate (Siegel et al., 2016). LSCC is prone to local infiltration and cervical lymph node metastasis, leading to difficult treatment and poor prognosis (Yuan et al., 2018; Gao et al., 2019). Therefore, it is urgent to find effective biomarkers for the diagnosis of LSCC.

Circular RNAs (circRNAs) are covalently closed non-coding RNA molecules that are more stable than linear RNA without 3' and 5' tails (Chen and Yang, 2015). In the study of cancer, circRNAs have been used as biomarkers of various cancer diseases due to their highly conserved and stable characteristics. In recent years, circRNAs have also been used in the study of LSCC. For example, Wu et al. found that circCORO1C is up-regulated in LSCC and plays a carcinogenic role (Wu et al., 2020). And Gao et al. demonstrated through a series of functional tests that circPARD3 can regulate the progression of LSCC by inhibiting autophagy (Gao et al., 2020). Similarly, Fan et al. demonstrated that circ_0044520 is upregulated in LSCC, but the function of circ_0044520 in LSCC has not been elucidated (Fan et al., 2018).

It has been shown that circRNAs serve as sponges for microRNAs (miRNAs) and play a competitive role with endogenous RNAs (ceRNAs) in tumor tissues (Hansen et al., 2013). MiRNAs can interact with the mRNA 3'UTR and exert a negative regulatory effect (Gregory and Shiekhattar, 2005; Macfarlane and Murphy, 2010). Many studies have shown that miR-338-

Corresponding Author: Huijun Yang, Department of Otolaryngology, First Affiliated Hospital of China Medical University, No.155, Nanjing North Street, Heping District, Shenyang City, Liaoning Province, China. e-mail: yanghuijun2004@163.com

DOI: 10.14670/HH-18-420

3p takes part in the occurrence and metastasis of LSCC. Li et al. found that miR-338-3p is targeted by Wee1 in laryngeal squamous cell carcinoma (Li et al., 2017). Jing et al. screened by GEO database and finally found that miR-338-3p can be used as a diagnostic marker of LSCC, but its function in LSCC has not been studied yet (Jing et al., 2020). Receptor tyrosine kinase orphan receptor 2 (ROR2) has also been determined to be up-regulated in various cancers, including head and neck squamous cell carcinoma (Kobayashi et al., 2009), but whether ROR2 is regulated by miR-338-3p and affects the development of LSCC remains unknown.

In this study, we found that circ_0044520 and ROR2 were up-regulated in LSCC tissues and cells. In addition, we testify to the role of circ_0044520/miR-338-3p/ROR2 axis in LSCC, in order to reveal the effect of circ_0044520 in the progression of LSCC.

Materials and methods

Patients' tissue

First Affiliated Hospital of China Medical University recruited 60 patients with LSCC to obtain tumor tissues and para-cancerous tissues. Pathological results of all individuals in both groups were reviewed. None of the patients had received chemotherapy or radiation. The tissue was immediately frozen in liquid nitrogen and stored at -80°C until RNA was extracted. All patients signed patient informed consent and were approved by First Affiliated Hospital of China Medical University.

Cell lines and Cell Transfection

Human Normal Oral Epithelial Keratinocytes (HOK), and Laryngeal squamous cell carcinoma cell line (SNU899 and TU177) were purchased from Cell Bank, Chinese Academy of Sciences (CAS, Shanghai, CHINA). All cell lines were cultured in DMEM medium containing 10% FBS (including 100 U/mL penicillin and 100 μg/mL streptomycin) in a cell incubator at 37°C with 5% CO_2 and 95% relative humidity. The cells at logarithmic growth stage were taken for experiment.

SNU899 and TU177 cells were conventionally cultured in the incubator and transfected when cell convergence reached 70%. Si-circ_0044520, si-NC, miR-338-3p mimic (miR-338-3p), miR-NC, miR-338-3p inhibitor (anti-miR-338-3p), anti-NC, pcDNA-ROR2 (ROR2) and pcDNA obtained from RiboBio (Guangzhou, China) were transfected into SNU899 and TU177 cells according to the transfection reagent instructions of Lipofectamine™ 2000 (Promega, Madison, WI, USA), respectively.

Quantitative real-time polymerase chain reaction (qRT-PCR)

Trizol reagent (Thermo Fisher, Waltham, MA, USA) was used to extract total RNA from LSCC tissues, paracancer tissues and SNU899 and TU177 cells in each transfection group. CDNA was synthesized by reverse transcription of total RNA using Reverse transcription kit (Thermo Fisher), and stored in a refrigerator at -20a. QRT-PCR reaction system was configured according to SYBR Green qRT-PCR Mix (Takara, Shiga, Japan) instructions. The expression levels of circ_0044520, ROR2 relative to internal reference GAPDH and miR-338-3p relative to U6 were calculated by $2^{-\Delta\Delta CT}$ method. The forward and reverse primers were displayed as below: GAPDH, (F: 5'- GGAGCGAGATCCCTCCA AAAT -3' and R: 5'- GGCTGTTGTCATACTTCTCA TGG -3'); U6, (F: 5'- CTCGCTTCGGCAGCACATATA CT -3' and R: 5'- ACGCTTCACGAATTTGCGTGTC -3'); circ_0044520, (F: 5'- TGCTCCTGGCAAAGATGG AC -3' and R: 5'- ACCAACAGCACCAGGGAAG -3'); miR-338-3p, (F: 5'- TGCGGTCCAGCATCAGTGAT -3' and R: 5'- CAGTGCGTGTCGTGGAGT -3'); ROR2, (F: 5'- AAGGAACCTCCCCAGCCA -3' and R: 5'- ACCACCCCTTTCTACGATGC -3').

Western blot analysis

The transfected SNU899 and TU177 cells were inoculated into 6-well plates (1.0×10^5 cells/well), and total protein was extracted with RIPA reagent after 48 h culture. After BCA quantification, electrophoresis, membrane transfer and sealing, anti-β-actin (1:1,000, ab8226, Abcam, Cambridge, MA, USA), anti-Proliferating Cell Nuclear Antigen (PCNA; 1:1,000, ab18197, Abcam), anti-cyclin D1 (1:200, ab16663, Abcam), anti-Bax (1:1,000, ab32503, Abcam), anti-Bcl-2 (1:1,000, ab692, Abcam) and anti-ROR2 (1:1,000, ab245456, Abcam) primary antibody were incubated overnight at 4□, respectively. After washing the film, goat anti-rabbit secondary antibody (1:1000, ab205718, Abcam) was used to incubate for 2 h at 37°C. The expression level of β-actin, PCNA, cyclin D1, Bax, Bcl-2 and ROR2 was analyzed by Image J software.

Cell counting Kit-8 assay

The transfected SNU899 and TU177 cells were inoculated into 96-well plates (2.5×10^4 cells/well) and cultured for 24, 48 and 72 h, respectively. Then 10 μL CCK-8 (Thermo Fisher) was added and incubated for 2 h. The OD value was measured at 450 nm using a microplate reader (BioTek, Winooski, Vermont, USA).

Colony formation assay

After transfection, SNU899 and TU177 cells in each group were inoculated into 6-well plates (1.0×10^4 cells/well), and fresh culture medium was changed once every 2 days.

After 14 days of culture, the culture medium was abandoned. After fixation with paraformaldehyde and crystal violet staining, the number of clones of more than

50 cells was counted under a microscope.

Flow cytometry assay

The Cell Cycle and Apoptosis of SNU899 and TU177 cells after transfection were analyzed according to the manufacturer's instructions of cell cycle and Apoptosis Analysis Kit (Beyotime, Shanghai, China) and flow cytometry (BD Biosciences, San Diego, CA, USA).

Tube formation assay

48-well plates were covered with Matrigel (BD Biosciences, USA). After matrigel curing for 1 h, 200 μL cell suspension was inoculated onto the gel. After incubation for 4-6 h, observation was made under a microscope and photos were taken. The ImageJ software (NIH, Bethesda, Maryland, USA) was used to quantify the tube formation.

Dual-luciferase reporter assay

Wild-type luciferase vectors of circ_0044520 or ROR2 3'UTR (WT-circ_0044520, WT-ROR2 3'UTR) and mutant luciferase vectors (MUT-circ_0044520, MUT-ROR2 3'UTR) were designed and synthesized by Shenggong Bioengineering Co., LTD (Shanghai, China). SNU899 and TU177 cells were inoculated into 6-well plates (1.0×10^5 cells/well). The above plasmids were co-transfected with miR-338-3p mimics or miR-NC by Lipofectamine™ 2000 liposome method, respectively. After transfection for 12 h, cells in each group were collected and lysed in fresh medium for another 24 h. After centrifugation at 3500 r/min for 5 min, the supernatant was taken and the luciferase activity was detected using Dual-Luciferase Reporter Assay Kit (GeneCopoeia, Rockville, MD, USA).

Xenograft models

All animal experiments were carried out in accordance with the instructions of First Affiliated Hospital of China Medical University Animal Care and Use Committee. TU177 cells were stably transfected with sh-NC or sh-circ_0044520. In tumor formation experiment, each mouse was subcutaneously injected with 2×10^6 cells or 200 μL PBS into BALB/C nude mice (6 weeks of age), purchased from Beijing Weidahe Laboratory Animal Science and Technology Co., Ltd. (Beijing, China). After one week of inoculation, the tumor volume was measured weekly and calculated by the formula: volume =1/2 (length×width^2). The mice were sacrificed 35 d after inoculation and the tumor was weighed.

Statistical analysis

All data were analyzed using GraphPad Prism 7 (GraphPad, San Diego, CA, USA) software and expressed as mean ± standard deviation. The significance of differences was assessed using Student's t-test or one-way ANOVA. $P<0.05$ was considered statistically significant.

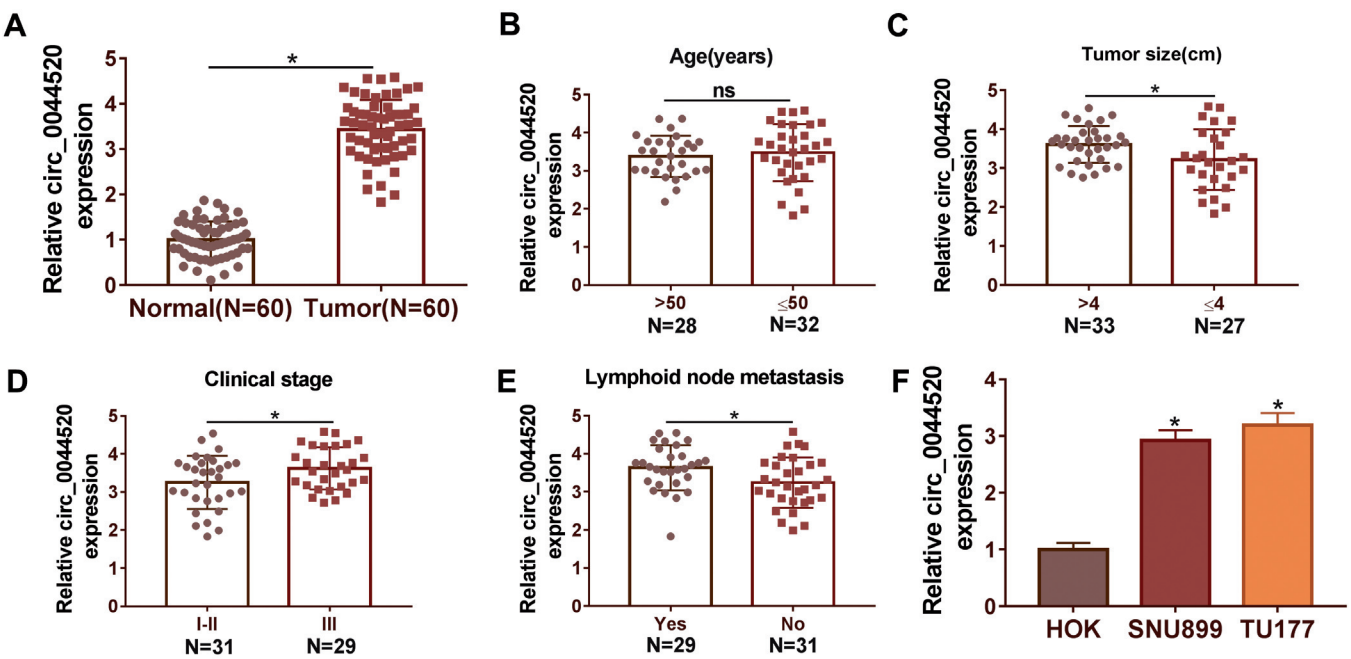

Fig. 1. Circ_0044520 was up-regulated in LSCC tissues and cell lines. **A-F.** QRT-PCR detected the expression of circ_0044520. *P<0.05.

Results

Circ_0044520 was up-regulated in LSCC tissues and cell lines

We first detected and analyzed LSCC tissues through qRT-PCR. As shown in Fig. 1A, the expression of circ_0044520 in LSCC tissues was higher than that in para-cancerous tissues. As shown in Fig. 1B-E, the expression of circ_0044520 was not correlated with age, but was correlated with tumor size, clinical stage, and lymphoid node metastasis. Finally, the expression of

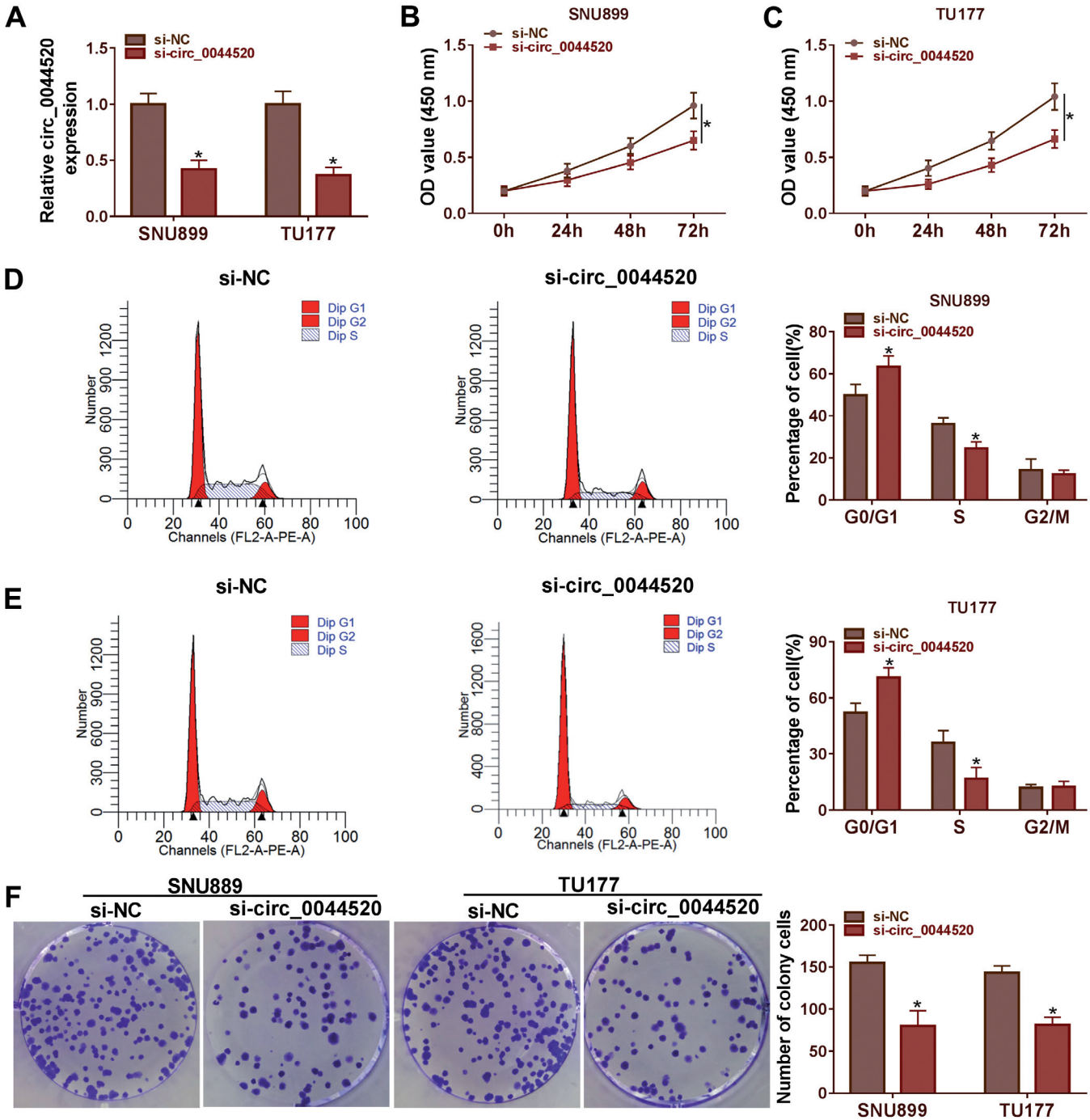

Fig. 2. The functional roles of si-circ_0044520 on proliferation and apoptosis in LSCC cells. **A.** The expression level of circ_0044520 was determined by qRT-PCR. **B, C.** CCK-8 was used to detect cell viability. **D, E.** Flow cytometry was used to detect cell cycle in transfected SNU899 and TU177 cells. **F.** Colony formation assay was used to assess proliferation of transfected SNU899 and TU177 cells. *P<0.05.

circ_0044520 in LSCC cell lines was detected by qRT-PCR, and it was found that the expression of circ_0044520 in LSCC cell lines was higher than that in non-cancer cell lines (Fig. 1F).

Silencing circ_0044520 inhibited the proliferation of LSCC cells

We further investigated the effect of circ_0044520 on LSCC cells by knocking down circ_0044520. As shown in Fig. 2A, the knockdown efficiency of circ_0044520 in SNU899 and TU177 cells was detected by qRT-PCR. Functionally, CCK-8 assay showed that si-circ_0044520 significantly inhibited the activity of LSCC cells (Fig. 2B,C). Flow cytometry showed that knocking down circ_0044520 significantly increased the percentage of SNU899 and TU177 cells in G0/G1 phase, while the percentage of S phase cells significantly decreased (Fig. 2D,E). Subsequently, the proliferation of transfected SNU899 and TU177 cells was measured by colony formation assay, and the results showed that knockdown of circ_0044520 significantly inhibited cell proliferation (Fig. 2F).

Silencing circ_0044520 promoted apoptosis of LSCC cells

Similarly, western blot analysis of proliferation-

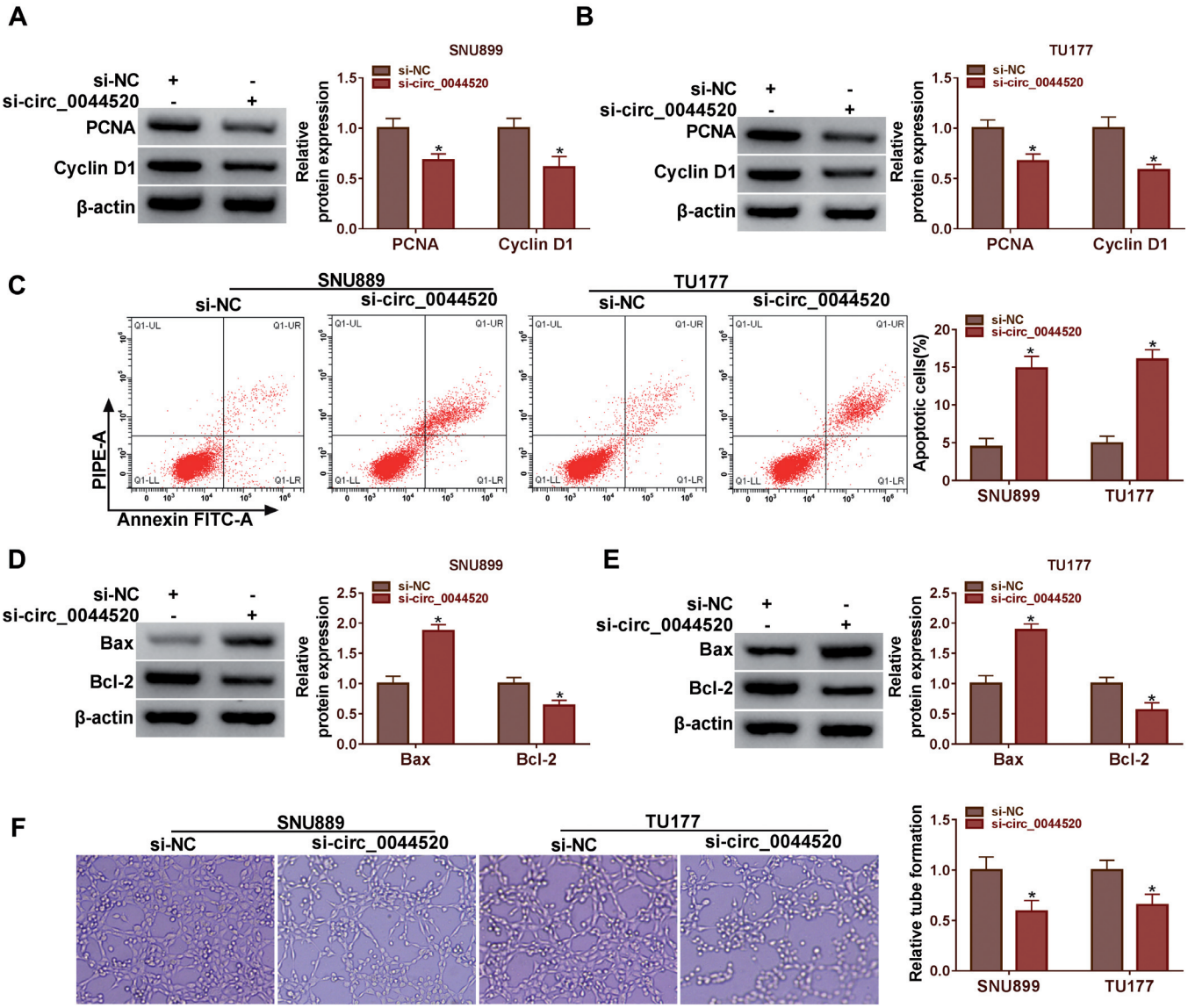

Fig. 3. The functional roles of si-circ_0044520 on apoptosis in LSCC cells. **A, B.** The expression level of PCNA and Cyclin D1 was determined by western blot. **C.** Flow cytometry was used to detect cell apoptosis. **D, E.** The expression level of Bax and Bcl-2 was determined by western blot. **F.** The angiogenesis test measures tube formation. *P<0.05.

related proteins showed that knockdown of circ_0044520 significantly reduced the expression of PNCA and Cyclin D1 in SNU899 and TU177 cells (Fig. 3A,B). Mechanically, knocking down circ_0044520 significantly promoted apoptosis in SNU899 and TU177 cells (Fig. 3C). Western blot analysis of apoptosis-related proteins showed that circ_0044520 knockdown significantly up-regulated the expression of Bax and decreased the expression of Bcl-2 (Fig. 3D,E). Finally, the angiogenesis assay showed that silencing circ_0044520 significantly reduced angiogenesis in SNU899 and TU177 cells (Fig. 3F). In general, silencing circ_0044520 significantly inhibited the malignant behavior of LSCC cells.

MiR-338-3p was the target of circ_0044520

Next, we predicted that circ_0044520 had a targeting relationship with miR-338-3p through StarBase3.0 (http://starbase.sysu.edu.cn/agoClipRNA.php?source=mRNA). Shown in Fig. 4A, is the binding site of circ_0044520 and miR-338-3p. Fig. 4B shows the overexpression efficiency of miR-338-3p as detected by qRT-PCR. Dual-luciferase reporter assay results showed that in SNU899 and TU177 cells, the combined transfection of miR-338-3p and circ_0044520-WT significantly inhibited luciferase activity, while the combined transfection of miR-338-3p and circ_0044520-MUT showed no significant change (Fig.

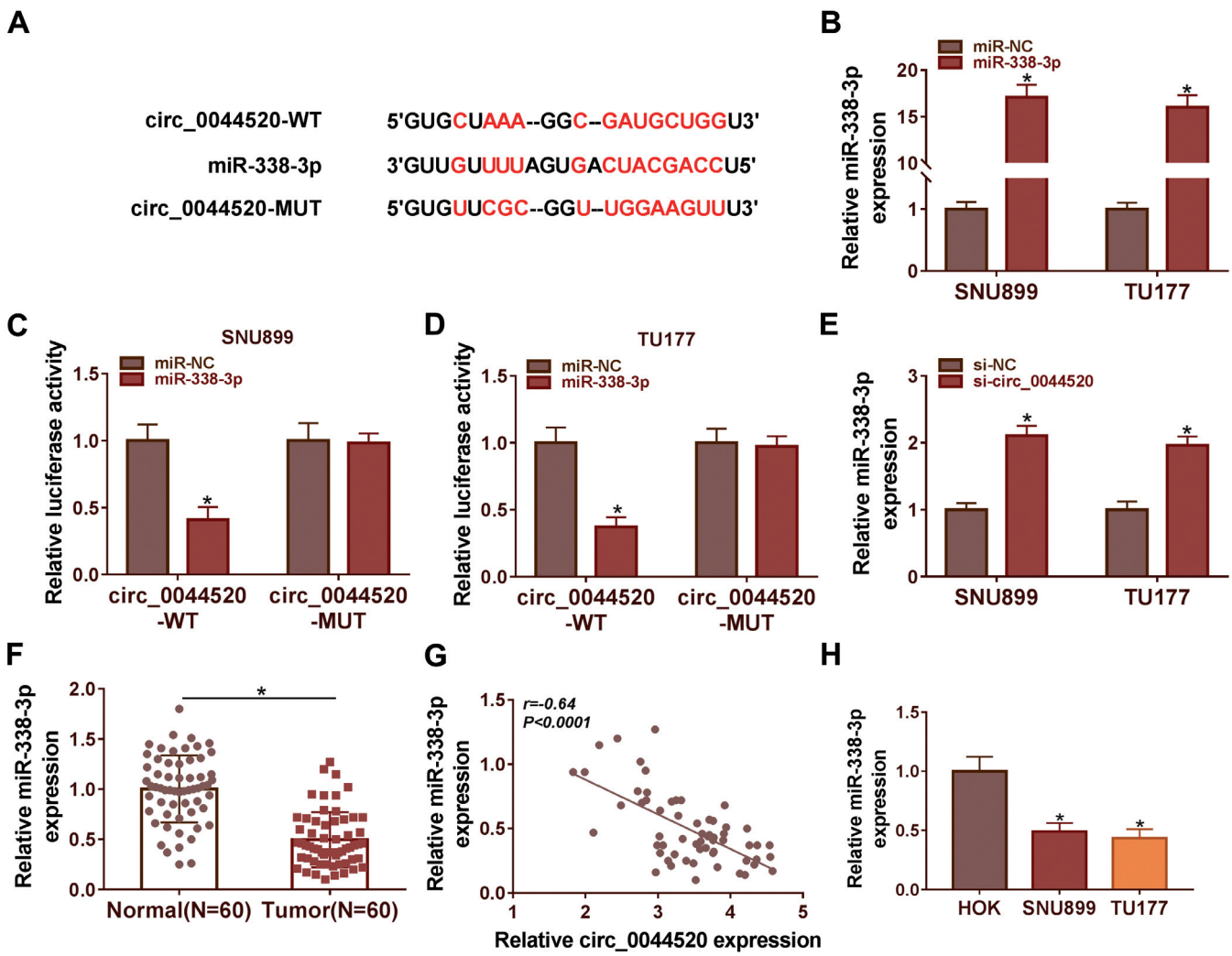

Fig. 4. Circ_0044520 functions as a sponge of miR-338-3p. **A.** The binding site of circ_0044520 and miR-338-3p was predicted with StarBase 3.0. **B, E.** The expression of miR-338-3p in transfected LSCC cells was tested by qRT-PCR. **C, D.** Dual-luciferase reporter assays were performed to confirm the association between miR-338-3p and circ_0044520. **F, H.** The expression of miR-338-3p in LSCC tissue (N=60) and cells was tested by qRT-PCR. **G.** Pearson's correlation analysis. *P<0.05.

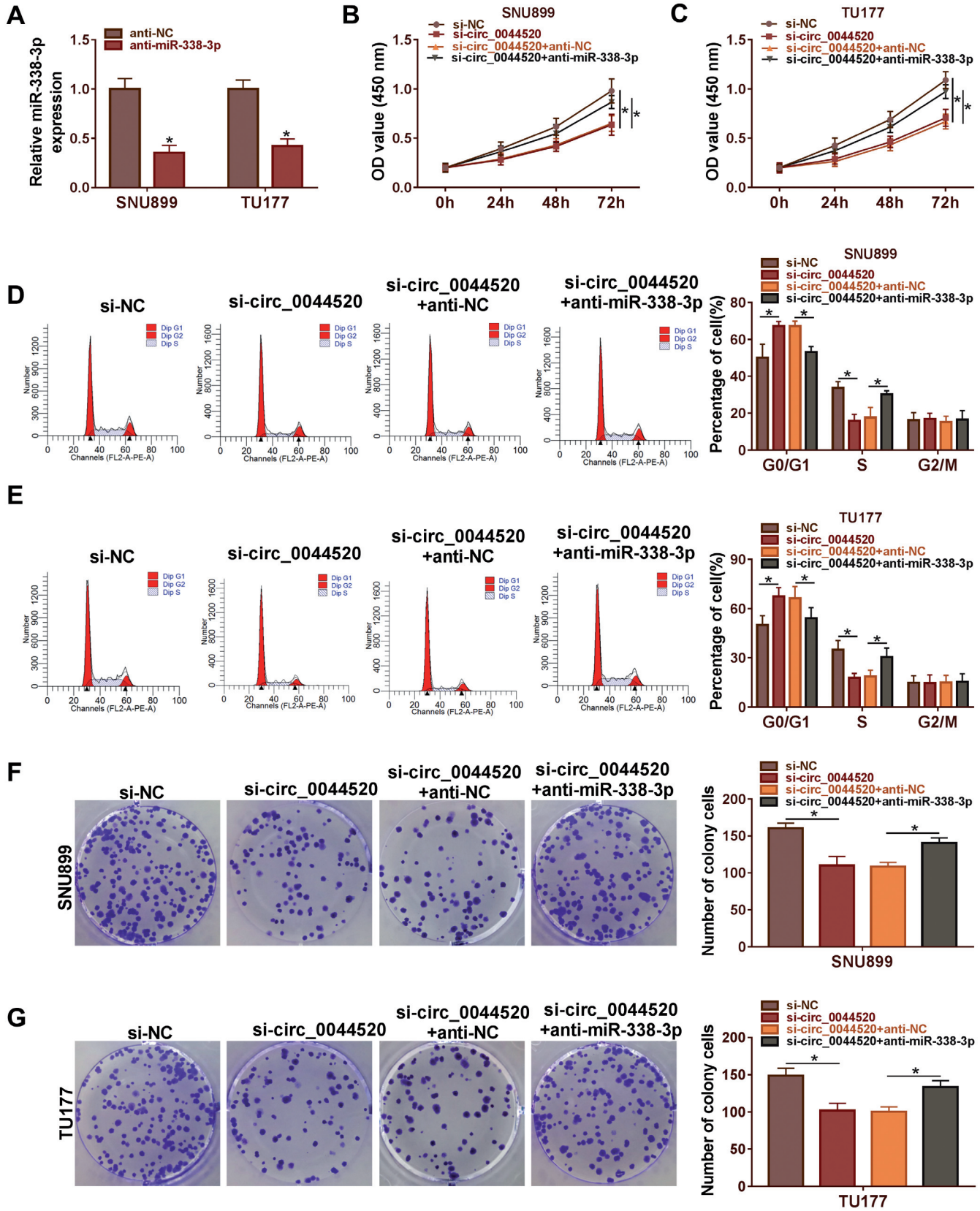

Fig. 5. Circ_0044520 regulated proliferation by targeting miR-338-3p in LSCC cells. **A.** The expression level of miR-338-3p was determined by qRT-PCR. **B, C.** CCK-8 assay was used to examine the cell viability. **D, E.** Flow cytometry was used to detect cell cycle in transfected SNU899 and TU177 cells. **F, G.** Colony formation assay was used to assess cell proliferation. *P<0.05.

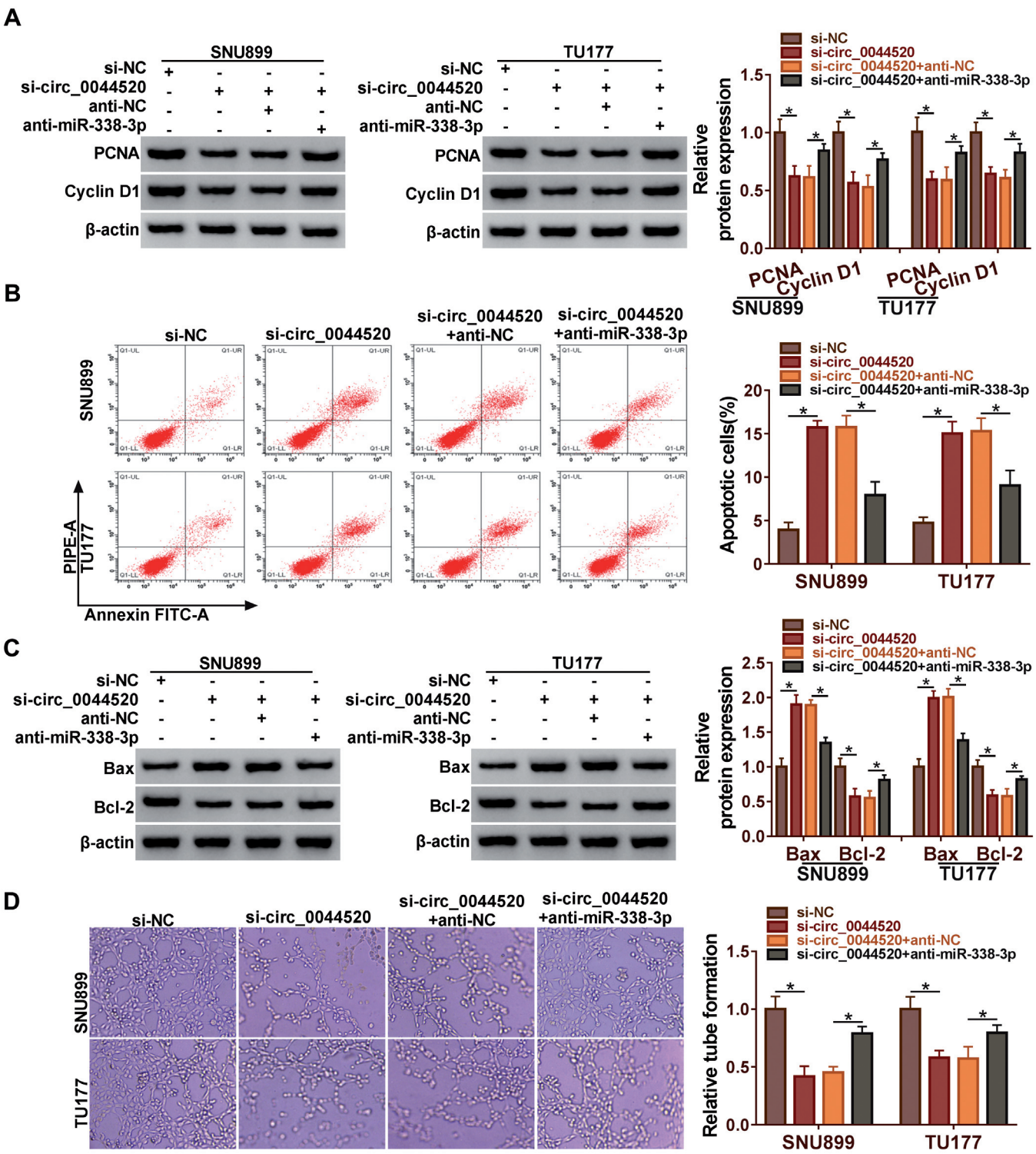

Fig. 6. Circ_0044520 regulated proliferation and apoptosis by targeting miR-338-3p in LSCC cells. **A.** The expression level of PCNA and Cyclin D1 was determined by western blot. **B.** Flow cytometry was used to detect cell apoptosis. **C.** The expression level of Bax and Bcl-2 was determined by western blot. **D.** The angiogenesis test measures tube formation. *P<0.05.

4C,D). QRT-PCR detection showed that knockdown of circ_0044520 significantly increased the expression of miR-338-3p (Fig. 4E), and Pearson's correlation analysis results showed that circ_0044520 was negatively correlated with miR-338-3p (Fig. 4G). QRT-PCR detected the low expression of miR-338-3p in LSCC cancer tissues and cell lines (Fig. 4F,H). In general, circ_0044520 was able to sponge miR-338-3p.

The miR-338-3p inhibitor reversed the effect of circ_0044520 knockdown on the proliferation inhibition of LSCC cells

In order to further explore whether circ_0044520 targeting miR-338-3p regulated the development of LSCC, we conducted a series of complement experiments. First, the transfection efficiency of miR-

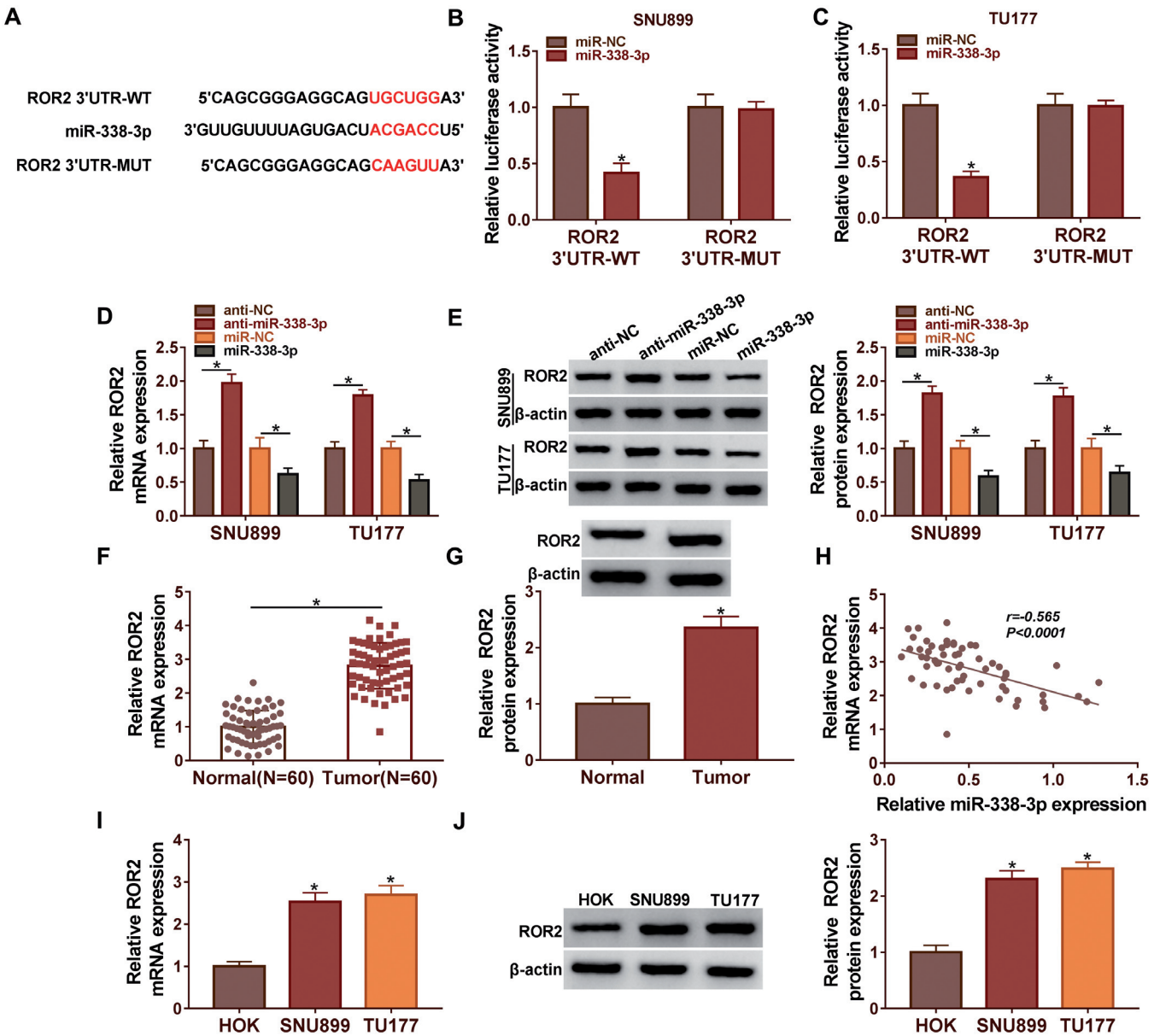

Fig. 7. ROR2 was the direct target of miR-338-3p. **A.** The binding site of ROR2 3'UTR and miR-338-3p was predicted with StarBase 3.0. **B, C.** Dual-luciferase reporter assays were performed to confirm the association between miR-338-3p and ROR2 3'UTR. **D.** The expression of ROR2 in transfected LSCC cells was tested by qRT-PCR. **E.** The expression of ROR2 in transfected LSCC cells was tested by western blot. **F, I.** The expression of ROR2 in LSCC tissue (N=60) and cells was tested by qRT-PCR. **G, J.** The expression of ROR2 in LSCC tissue (N=60) and cells was tested by western blot. **H.** Pearson's correlation analysis. *P<0.05.

338-3p inhibitor was detected by qRT-PCR (Fig. 5A). Next, CCK-8 assay showed that miR-338-3p inhibitor was able to significantly restore the viability of SNU899 and TU177 cells inhibited by si-circ_0044520 (Fig. 5B,C). Flow cytometry results showed that miR-338-3p inhibitor was able to recover the effect of si-circ_0044520 on SNU899 and TU177 cells blocked in the G0/G1 phase (Fig. 5D,E). Functionally, the results of clone formation assay showed that anti-miR-338-3p was able to up-regulate cell proliferation inhibited by circ_0044520 silencing (Fig. 5F,G).

The miR-338-3p inhibitor reversed the effect of circ_0044520 knockdown on the apoptosis promotion of LSCC cells

Western blot results showed that anti-miR-338-3p up-regulated the expression of PCNA and Cyclin D1 proteins inhibited by circ_0044520 silencing (Fig. 6A). Mechanically, anti-miR-338-3p inhibited apoptosis of SNU899 and TU177 cells up-regulated by si-circ_0044520 (Fig. 6B). Also, the up-regulation of Bax and down-regulation of Bcl-2 by si-circ_0044520 was reversed by miR-338-3p inhibitor (Fig. 6C). In addition, si-circ_0044520 inhibited tube formation in LSCC cells, while co-transfection with miR-338-3p inhibitor was able to partially reverse it (Fig. 6D). In a word, circ_0044520 played a regulatory role in LSCC cells by sponging miR-338-3p.

ROR2 was the target of MiR-338-3p

Next, we predicted that miR-338-3p had a targeting relationship with ROR2 through StarBase3.0 (http://starbase.sysu.edu.cn/agoClipRNA.php?source=mRNA). Shown in Fig. 7A is the binding site of ROR2

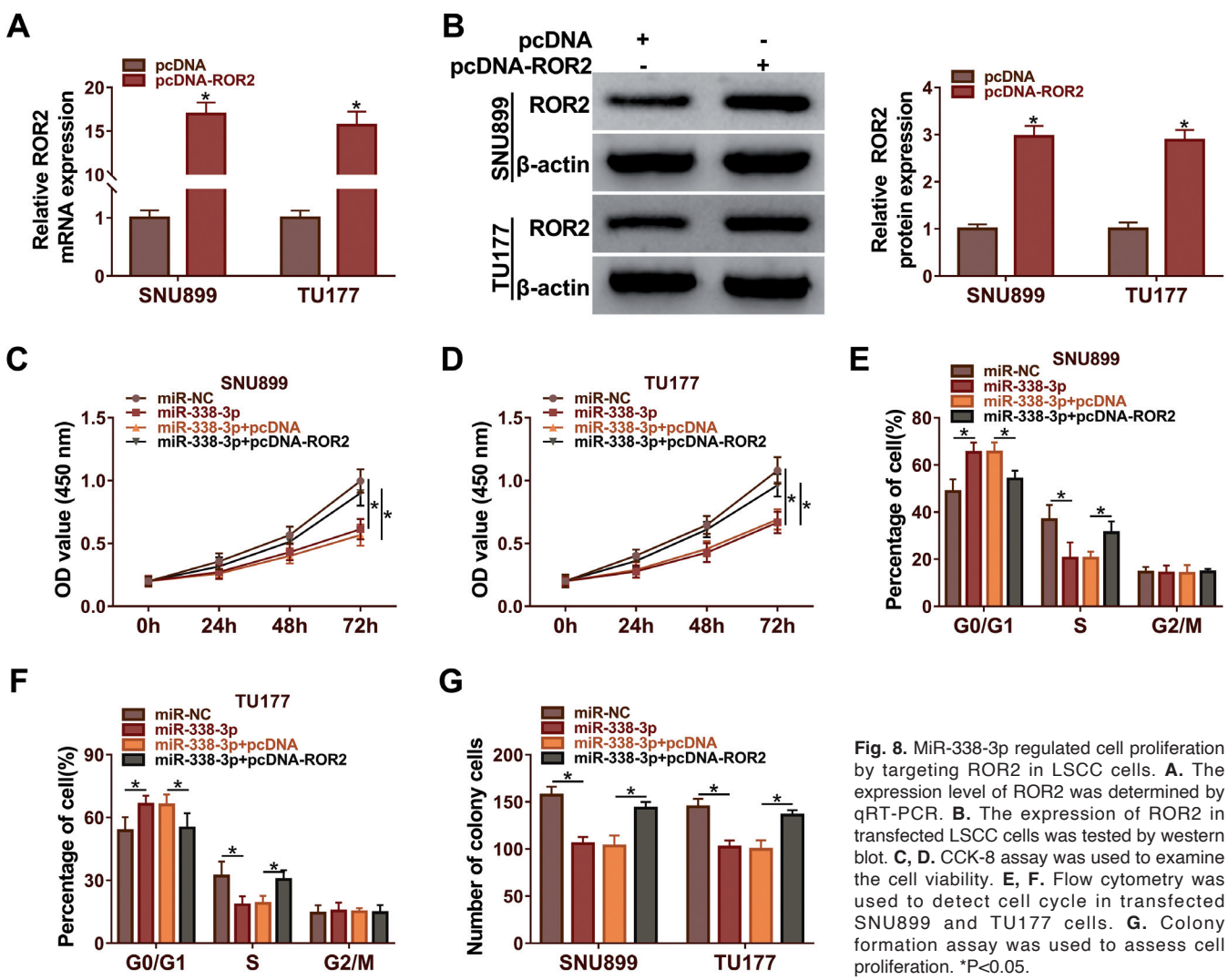

Fig. 8. MiR-338-3p regulated cell proliferation by targeting ROR2 in LSCC cells. **A.** The expression level of ROR2 was determined by qRT-PCR. **B.** The expression of ROR2 in transfected LSCC cells was tested by western blot. **C, D.** CCK-8 assay was used to examine the cell viability. **E, F.** Flow cytometry was used to detect cell cycle in transfected SNU899 and TU177 cells. **G.** Colony formation assay was used to assess cell proliferation. *P<0.05.

3'UTR and miR-338-3p. Dual-luciferase reporter assay results showed that in SNU899 and TU177 cells, the co-transfection of miR-338-3p and ROR2 3'UTR-WT significantly inhibited luciferase activity, while the co-transfection of miR-338-3p and ROR2 3'UTR-MUT showed no significant change (Fig. 7B,C). Next, qRT-PCR and western blot were used to detect the changes in ROR2 expression after transfection with miR-338-3p inhibitor or overexpression of miR-338-3p in SNU899 and TU177 cells. The results showed that miR-338-3p inhibitors significantly up-regulated the expression of ROR2, while overexpression of miR-338-3p can significantly down-regulate the expression of ROR2 (Fig. 7D,E). QRT-PCR (Fig. 7F,I) and western blot (Fig. 7G,J) detected the high expression of ROR2 in LSCC cancer tissues and cell lines. In general, ROR2 was a direct target of miR-338-3p. Pearson's correlation analysis results showed that ROR2 was negatively correlated with miR-338-3p (Fig. 7H).

Overexpression of ROR2 reversed the effect of miR-338-3p on the proliferation and cell cycle of LSCC cells

Next, we verified whether there was a regulatory relationship between miR-338-3p and ROR2 in LSCC. First, the transfection efficiency of ROR2 overexpressed vector was detected by qRT-PCR and western blot (Fig. 8A,B). Next, CCK-8 assay showed that overexpression of ROR2 was able to significantly restore the viability of SNU899 and TU177 cells inhibited by miR-338-3p (Fig. 8C,D). Flow cytometry results showed that pcDNA-ROR2 was able to recover the effect of miR-338-3p on SNU899 and TU177 cells blocked in the G0/G1 phase (Fig. 8E,F). Functionally, the results of clone formation assay showed that pcDNA-ROR2 was able to up-regulate cell proliferation inhibited by miR-338-3p (Fig. 8G).

Overexpression of ROR2 reversed the effect of miR-338-3p on the apoptosis of LSCC cells

Overexpression of ROR2 up-regulated the expression of PCNA and Cyclin D1 proteins inhibited by miR-338-3p (Fig. 9A,B). Moreover, pcDNA-ROR2 inhibited apoptosis of SNU899 and TU177 cells up-regulated by miR-338-3p (Fig. 9C). Also, Western blot analysis showed that pcDNA-ROR2 reversed the up-regulation of Bax and down-regulation of Bcl-2 by miR-338-3p (Fig. 9D,E). Lastly, overexpression of miR-338-3p inhibited tube formation in LSCC cells, while co-transfection with pcDNA-ROR2 was able to partially reverse it (Fig. 9F). Taken together, pcDNA-ROR2

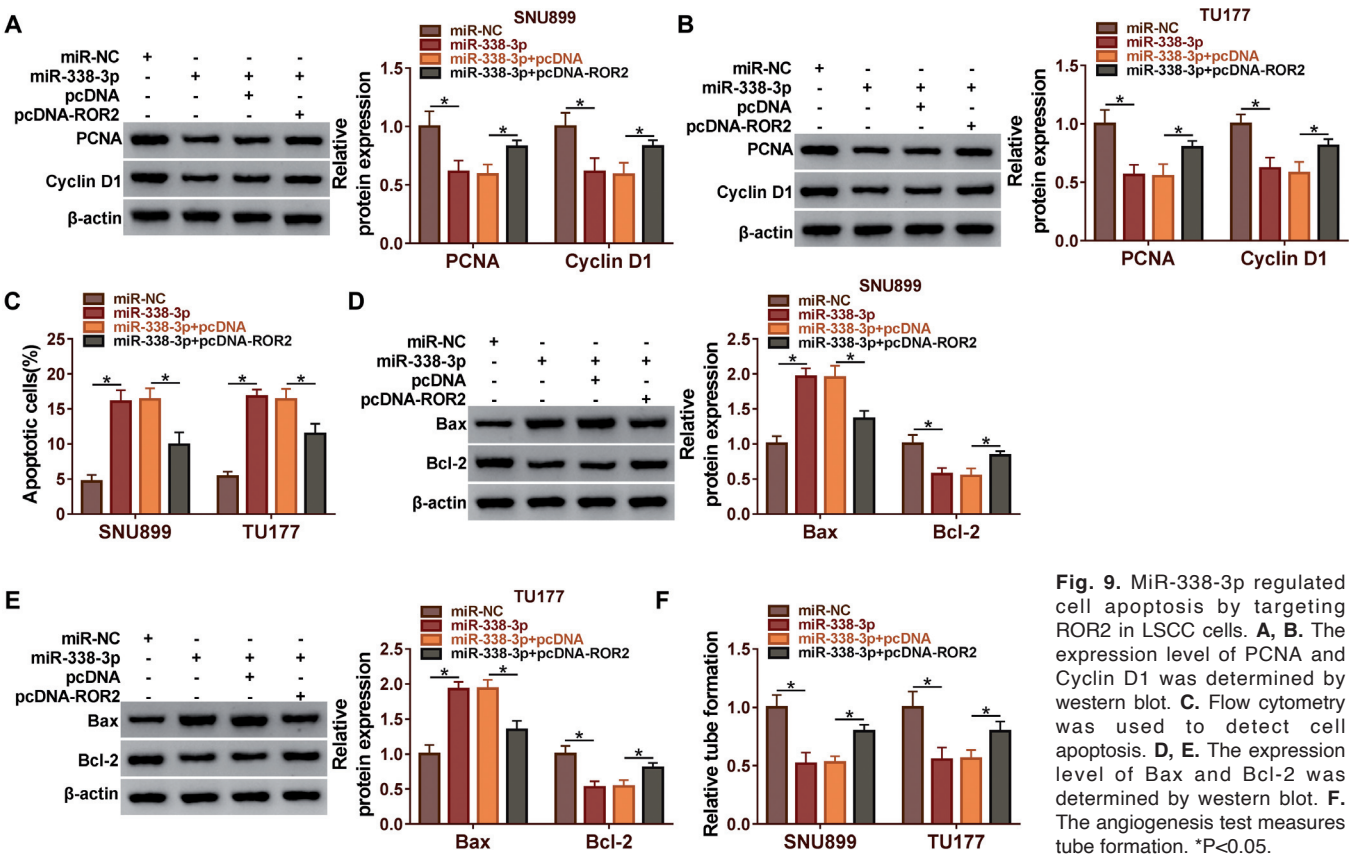

Fig. 9. MiR-338-3p regulated cell apoptosis by targeting ROR2 in LSCC cells. **A, B.** The expression level of PCNA and Cyclin D1 was determined by western blot. **C.** Flow cytometry was used to detect cell apoptosis. **D, E.** The expression level of Bax and Bcl-2 was determined by western blot. **F.** The angiogenesis test measures tube formation. *P<0.05.

reversed the effect of overexpression of miR-338-3p in LSCC cells.

Circ_0044520 regulated the expression of ROR2 via miR-338-3p

Pearson's correlation analysis showed that circ_0044520 was positively correlated with ROR2 (Fig. 10A). QRT-PCR and western blot analysis showed that knockdown of circ_0044520 was able to significantly down-regulate the expression of ROR2, while miR-338-3p inhibitor was able to partially up-regulate the expression of ROR2 (Fig. 10B,C).

Circ_0044520 knockdown inhibited tumor growth in vivo

Next, we explored the effect of circ_0044520 on LSCC in vivo by constructing a xenograft model. By measuring tumor volume weekly, we found that silencing circ_0044520 significantly increased tumor volume (Fig. 11A). Similarly, sh-circ_0044520 inhibited tumor weight (Fig. 11B). Subsequently, qRT-PCR results showed that knockdown of circ_0044520 significantly reduced circ_0044520 levels, and up-regulated miR-338-3p expression (Fig. 11C,D). In addition, sh-circ_0044520 significantly decreased the expression of ROR2 (Fig. 11E,F). In conclusion, knockdown of circ_0044520 inhibited tumor growth.

Discussion

Extensive research emphasized that the crosstalk of circRNAs as ceRNA via shared miRNAs was involved in the pathogenesis of human diseases, including cancer (Arnaiz et al., 2019). New experimental evidence suggested that circRNAs have ceRNA activity in the development of laryngeal squamous cell carcinoma (Lu et al., 2018). However, understanding the precise role of circRNA-mediated ceRNA networks in the progression of LSCC had been a challenge. Here, we demonstrated for the first time the role of circ_0044520 as a novel regulator of functional characterization of LSCC cells by regulating the miR-338-3p/ROR2 axis.

Our results showed that circ_0044520 was highly-expressed in LSCC tissues and cells. This result was consistent with previous findings, for example, maladjustment of circ_0000218 and circ_0067934 in LSCC was involved in miRNA competition (Bai et al., 2020; Chu, 2020). In this study, the role of circ_0044520 in LSCC cell lines SNU899 and TU177 was investigated by functional cell assay. The results showed that si-circ_0044520 inhibited the cell viability

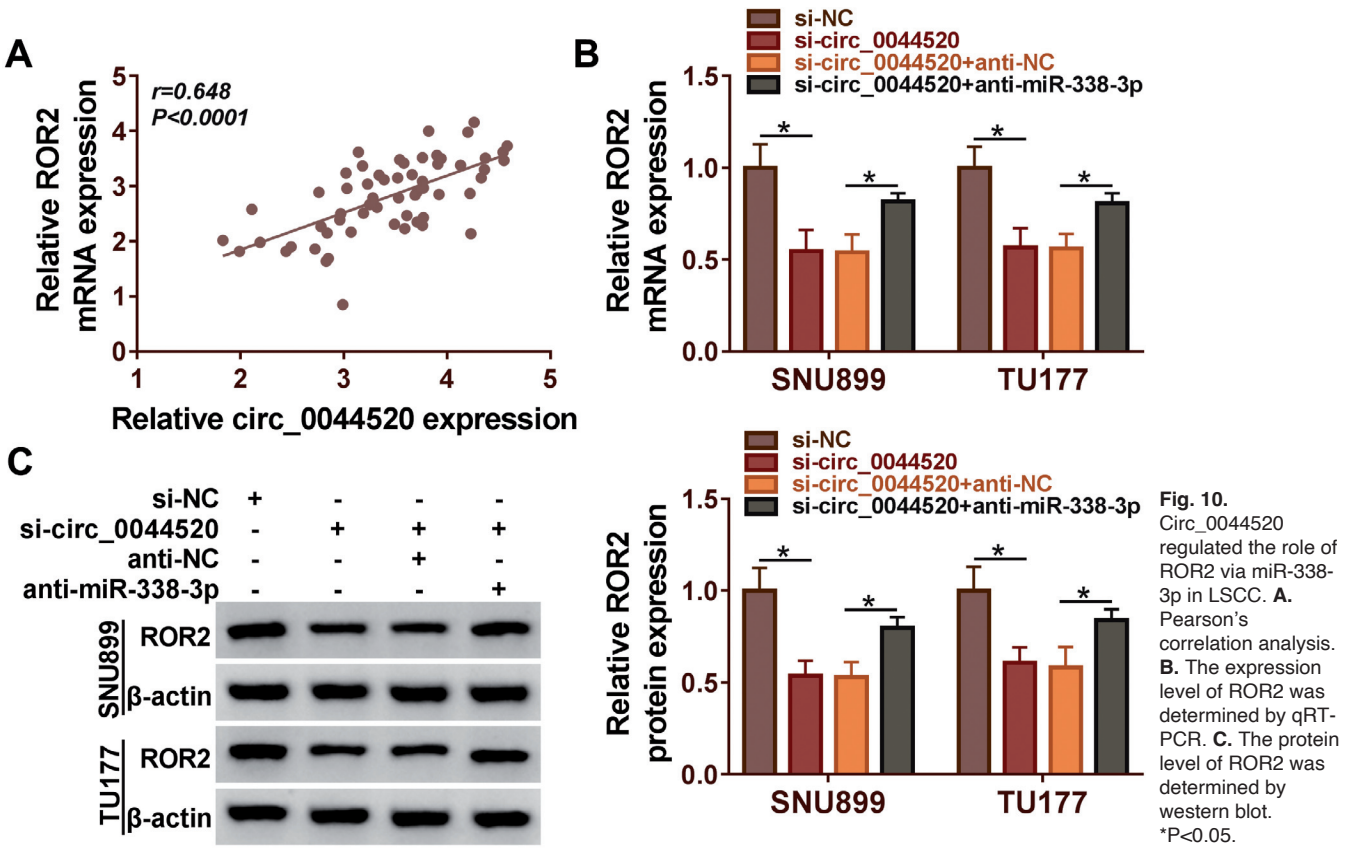

Fig. 10. Circ_0044520 regulated the role of ROR2 via miR-338-3p in LSCC. **A.** Pearson's correlation analysis. **B.** The expression level of ROR2 was determined by qRT-PCR. **C.** The protein level of ROR2 was determined by western blot. *P<0.05.

and proliferation of SNU899 and TU177 cells, and promoted cell apoptosis. Current studies have found that angiogenesis was one of the hallmarks of tumors, which promoted the growth and development of tumors. Using an angiogenesis assay, we demonstrated for the first time that circ_0044520 silences angiogenesis in LSCC cells. This suggested that tumor angiogenesis inhibition from knocking down circ_0044520 could be used as a therapeutic strategy for the treatment of LSCC. Similarly, circ_0044520 silencing also inhibited LSCC growth in vivo. It is worth mentioning that our study showed that circ_0044520 played a role in LSCC cells by regulating the expression of miR-338-3p.

A large number of studies have demonstrated that miR-338-3p has anti-tumor activity in human cancers such as hepatocellular carcinoma, gastric carcinoma and osteosarcoma (Lu et al., 2020; Zhang et al., 2020; Kuai et al., 2021). Our results confirmed that miR-338-3p was an effective tumor inhibitor in LSCC, which was consistent with the results of previous studies. In addition, we investigated the regulatory role of miR-338-3p and circ_0044520 in the occurrence of LSCC through functional cell complement assay. The results showed that miR-338-3p inhibitor was able to restore the inhibitory effect of circ_0044520 on the malignant behavior of LSCC cells. We also found that ROR2 was a direct and functional target of miR-338-3p. Consistent with the results of Zhang et al., we found that ROR2 was significantly overexpressed in LSCC (Zhang et al., 2017). More importantly, we showed that the ceRNA activity of circ_0044520 regulated ROR2 expression through shared miR-338-3p.

In summary, circ_0044520 was established here as a new regulator of LSCC progression. We discovered a novel circ_0044520/miR-338-3p/ROR2 regulatory network in the development of LSCC. Therefore, the circ_0044520 inhibitor appeared to be a promising candidate for the development of new antitumor therapies.

Acknowledgements. None

Disclosure of interest. The authors declare that they have no conflicts of interest

Funding. None.

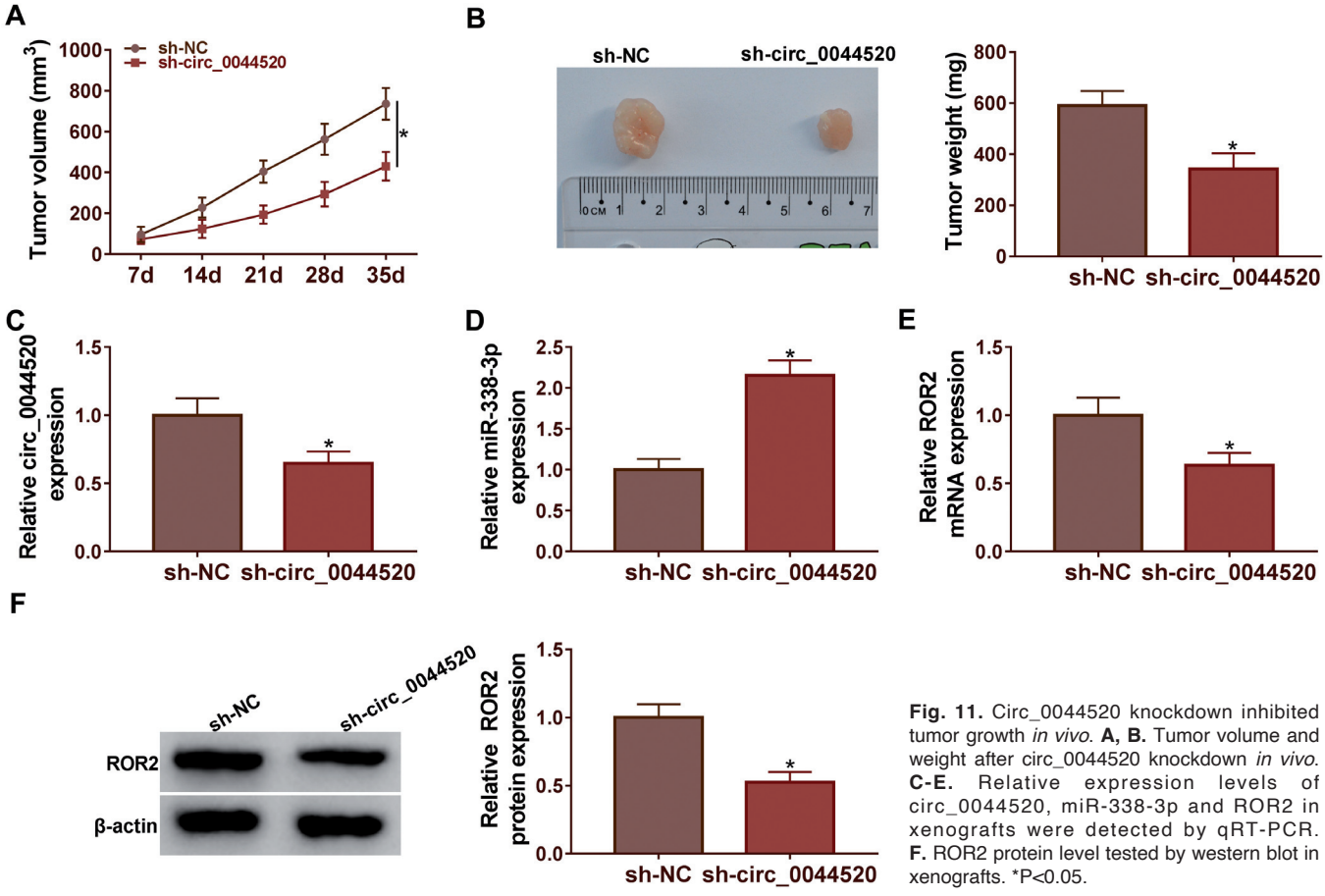

Fig. 11. Circ_0044520 knockdown inhibited tumor growth *in vivo*. **A, B.** Tumor volume and weight after circ_0044520 knockdown *in vivo*. **C-E.** Relative expression levels of circ_0044520, miR-338-3p and ROR2 in xenografts were detected by qRT-PCR. **F.** ROR2 protein level tested by western blot in xenografts. *P<0.05.

References

Arnaiz E., Sole C., Manterola L., Iparraguirre L., Otaegui D. and Lawrie C.H. (2019). CircRNAs and cancer: Biomarkers and master regulators. Semin. Cancer Biol. 58, 90-99.

Bai Y., Hou J., Wang X., Geng L., Jia X., Xiang L. and Nan K. (2020). Circ_0000218 plays a carcinogenic role in laryngeal cancer through regulating microRNA-139-3p/Smad3 axis. Pathol. Res. Pract. 216, 153103.

Chen L.L. and Yang L. (2015). Regulation of circRNA biogenesis. RNA Biol. 12, 381-388.

Chu Y.L. (2020). Circ_0067934 correlates with poor prognosis and promotes laryngeal squamous cell cancer progression by sponging miR-1324. Eur. Rev. Med. Pharmacol. Sci. 24, 4320-4327.

Fan Y., Xia X., Zhu Y., Diao W., Zhu X., Gao Z. and Chen X. (2018). Circular RNA expression profile in laryngeal squamous cell carcinoma revealed by microarray. Cell Physiol. Biochem. 50, 342-352.

Gao W., Guo H., Niu M., Zheng X., Zhang Y., Xue X., Bo Y., Guan X., Li Z., Guo Y., He L., Zhang Y., Li L., Cao J. and Wu Y. (2020). circPARD3 drives malignant progression and chemoresistance of laryngeal squamous cell carcinoma by inhibiting autophagy through the PRKCI-Akt-mTOR pathway. Mol. Cancer 19, 166.

Gao W., Zhang Y., Niu M., Bo Y., Li H., Xue X., Lu Y., Zheng X., Tang Y., Cui J., He L., Thorne R.F., Wang B. and Wu Y. (2019). Identification of miR-145-5p-centered competing endogenous RNA network in laryngeal squamous cell carcinoma. Proteomics 19, e1900020.

Gregory R.I. and Shiekhattar R. (2005). MicroRNA biogenesis and cancer. Cancer Res. 65, 3509-3512.

Hansen T.B., Kjems J. and Damgaard C.K. (2013). Circular RNA and miR-7 in cancer. Cancer Res. 73, 5609-5612.

Jing Z., Guo S., Zhang P. and Liang Z. (2020). LncRNA-associated cerna network reveals novel potential biomarkers of laryngeal squamous cell carcinoma. Technol. Cancer Res. Treat. 19, 1533033820985787.

Kobayashi M., Shibuya Y., Takeuchi J., Murata M., Suzuki H., Yokoo S., Umeda M., Minami Y. and Komori T. (2009). Ror2 expression in squamous cell carcinoma and epithelial dysplasia of the oral cavity. Oral Surg. Oral Med. Oral Pathol. Oral Radiol. Endod. 107, 398-406.

Kuai J., Zheng L., Yi X., Liu Z., Qiu B., Lu Z. and Jiang Y. (2021). ST8SIA6-AS1 promotes the development of hepatocellular carcinoma cells through miR-338-3p/NONO Axis. Dig. Liver Dis. 53, 1192-1200.

Li P., Yang Y., Liu H., Yang A.K., Di J.M., Tan G.M., Wang H.F., Qiu J.G., Zhang W.J., Jiang Q.W., Zheng D.W., Chen Y., Wei M.N., Huang J.R., Wang K., Shi Z. and Ye J. (2017). miR-194 functions as a tumor suppressor in laryngeal squamous cell carcinoma by targeting Wee1. J. Hematol. Oncol. 10, 32.

Lu C., Shi X., Wang A.Y., Tao Y., Wang Z., Huang C., Qiao Y., Hu H. and Liu L. (2018). RNA-Seq profiling of circular RNAs in human laryngeal squamous cell carcinomas. Mol. Cancer 17, 86.

Lu H., Zhang Q., Sun Y., Wu D. and Liu L. (2020). LINC00689 induces gastric cancer progression via modulating the miR-338-3p/HOXA3 axis. J. Gene Med. 22, e3275.

Macfarlane L.A. and Murphy P.R. (2010). MicroRNA: Biogenesis, function and role in cancer. Curr. Genomics 11, 537-561.

Siegel R.L., Miller K.D. and Jemal A. (2015). Cancer statistics, 2015. CA Cancer J. Clin. 65, 5-29.

Siegel R.L., Miller K.D. and Jemal A. (2016). Cancer statistics, 2016. CA Cancer J. Clin. 66, 7-30.

Steuer C.E., El-Deiry M., Parks J.R., Higgins K.A. and Saba N.F. (2017). An update on larynx cancer. CA Cancer J. Clin. 67, 31-50.

Wu Y., Zhang Y., Zheng X., Dai F., Lu Y., Dai L., Niu M., Guo H., Li W., Xue X., Bo Y., Guo Y., Qin J., Qin Y., Liu H., Zhang Y., Yang T., Li L., Zhang L., Hou R., Wen S., An C., Li H., Xu W. and Gao W. (2020). Circular RNA circCORO1C promotes laryngeal squamous cell carcinoma progression by modulating the let-7c-5p/PBX3 axis. Mol. Cancer 19, 99.

Yuan Z., Xiu C., Song K., Pei R., Miao S., Mao X., Sun J. and Jia S. (2018). Long non-coding RNA AFAP1-AS1/miR-320a/RBPJ axis regulates laryngeal carcinoma cell stemness and chemoresistance. J. Cell Mol. Med. 22, 4253-4262.

Zhang H., Wang J., Ren T., Huang Y., Yu Y., Chen C., Huang Q. and Guo W. (2020). LncRNA CASC15 is upregulated in osteosarcoma plasma exosomes and CASC15 knockdown inhibits osteosarcoma progression by regulating miR-338-3p/RAB14 axis. Onco Targets Ther. 13, 12055-12066.

Zhang W., Yan Y., Gu M., Wang X., Zhu H., Zhang S. and Wang W. (2017). High expression levels of Wnt5a and ROR2 in laryngeal squamous cell carcinoma are associated with poor prognosis. Oncol. Lett. 14, 2232-2238.

Accepted January 17, 2022